

A. N. Tarashchan · M. N. Taran · H. Rager · W. Iwanuch

Luminescence spectroscopic study of Cr³⁺ in Brazilian topazes from Ouro Preto

Received: 19 April 2005 / Accepted: 21 September 2005 / Published online: 6 December 2005
© Springer-Verlag 2005

Abstract In this paper, the results of investigation of luminescent properties of topazes from Ouro Preto, Brazil are presented. It is established that all photoluminescence characteristics of variously colored topazes are due to three structurally non-equivalent Cr³⁺ centers isomorphically substituting Al³⁺ in the topaz structure and forming [CrO₄F₂]⁷⁻, [CrO₄OH,F]⁷⁻, and [CrO₄(OH)₂]⁷⁻ complexes. Kinetics of thermal annealing indicates different thermal stability of these centers. Less stable [CrO₄OH, F]⁷⁻ and [CrO₄(OH)₂]⁷⁻ complexes diminish in temperature range 950–1,100°C, accompanied by appearance of corundum phase. The most stable [CrO₄F₂]⁷⁻ centers completely decay at 1,250°C and luminescence spectrum of product obtained becomes identical to that of Cr³⁺ in mullite indicating that topaz completely transforms to mullite.

Keywords Topaz · Chromium · Luminescence · Phase transitions

Introduction

Trivalent chromium, Cr³⁺, is the most stable state of chromium and, therefore, widely spread in minerals producing deep colors and bright photoluminescence. For instance, the color of many natural and synthetic gemstones like ruby, emerald, alexandrite, etc., is caused by Cr³⁺. On this account, Cr³⁺ is subject of numerous optical spectroscopic and luminescence investigations. Further, Cr³⁺-bearing crystals are used in modern technologies, for example, as solid-state laser materials. Local properties of Cr³⁺ in minerals like crystal field stabilization energy, symmetry, interatomic distances, covalency/ionicity of Cr–O bonds have been studied in great detail (e.g., Burns 1993 and literature cited therein). This interest is additionally enhanced by the fact that some Cr³⁺-bearing phases are important constituents of the deep-seated mantle rocks.

Spectroscopic studies of chromium-bearing varieties of the silicate mineral topaz, Al₂(F,OH)₂SiO₄, are interesting because the sixfold ligand surrounding of Cr³⁺ varies with F⁻ to hydroxyl substitution, the degree of which is different and depends significantly on the deposit. The OH/OH + F ratio in natural topazes varies from 0 to nearly 30%. Due to non-random F⁻ to OH-substitution the orthorhombic symmetry of topaz structure may decrease to monoclinic or even to triclinic (Akizuki et al. 1979; Parise et al. 1980). F↔OH substitution noticeably distorts the local crystal field of Cr³⁺ centers and, hence, influences optical absorption (Taran et al. 2003) and luminescence spectra (Tarashchan 1978) of natural topazes. Therefore, this system is of a great interest to be studied spectroscopically.

Luminescence of topaz has been investigated only fragmentarily. Deutschbein (1932) reported luminescence lines in the red part of the visible range at room temperature and 77 K. Tarashchan (1978) attributed some features of the steady-state luminescence of topaz to both isolated and paired Cr³⁺ ions. Gaft et al. (2003) recently studied laser-induced time-resolved fluorescence

A. N. Tarashchan (✉) · M. N. Taran
Institute of Geochemistry, Mineralogy and Ore Formation,
National Academy of Sciences of Ukraine,
Paladin Avenue 34, 03680 Kyiv-142, Ukraine
E-mail: taran@igmof.gov.ua
Tel.: + 38-44-4240043
Fax: + 38-44-4241270

H. Rager
Fachbereich Geowissenschaften, Philipps-Universität Marburg,
35032 Marburg, Germany
E-mail: rager@mail.uni-marburg.de

W. Iwanuch
Departamento de Química Fundamental,
Laboratório dos elementos do Bloco,
Universidade de São Paulo, f. Av. Prof. Lineo Prestes,
748, Bloco 8-T, 05508-900 São Paulo, SP, Brasil
E-mail: wold@uol.com.br

spectra of Cr^{3+} in natural topazes which were attributed likewise to isolated Cr^{3+} and $\text{Cr}^{3+}-\text{Cr}^{3+}$ pairs as well as to radiation-induced centers associated with chromium. Further, different effects like non-homogeneous distribution of chromium ions, luminescence centers of different crystal field strength and symmetry which in turn are due to various isomorphous substitutions, extraordinary strong splitting of electronic levels of Cr^{3+} , etc., reveal individual features in experimental luminescence spectra. To the best of our knowledge these features have not been studied in detail until now.

In this paper, the luminescence of natural gem quality chromium bearing topazes from Ouro Preto, Minas Gerais, Brasil is reported. Special attention has been paid to the influence of low local symmetry and different local distortions of the Cr^{3+} centers on the luminescence and excitation spectra to justify independently non-equivalent Cr^{3+} centers in the topaz structure as reported by Taran et al. (2003). The transformation of these centers by a high-temperature treatment of topaz was another concern. Therefore, the photoluminescence of variously colored Cr-bearing natural topazes annealed at different temperatures was investigated as well as the luminescence excitation spectra at room temperature and 77 K. Moreover, the kinetic of thermal bleaching of natural and irradiated topazes and the effects of annealing were studied on the basis of characteristic luminescence features.

Experimental details

The investigation was performed on six topaz crystals, K1–K6, recently studied by Taran et al. (2003). K1–K4 are differently colored crystals from Saramenha and K5 is a colorless topaz from Rodrigo Silva. K1–K5 are topazes from Ouro Preto, Brazil. K6, a deep-violet topaz from Kamenka, Ural (Russia) of extremely high chromium content, 0.36 wt% Cr_2O_3 , was studied for comparison. Large single crystals sometimes with several centimeters side length were examined under a binocular and a polarizing microscope. Then, samples free from inclusions or other visible defects were cut from a uniformly colored zone of the crystals. However, the observed intensity distribution of the Cr photoluminescence suggests that even in such carefully selected samples chromium is distributed inhomogeneously in agreement with microprobe data of similar samples from Brazilian deposits reported by Schott et al. (2003).

For the luminescence measurements the samples were prepared as polished parallelepipeds of ca. $3 \times 3 \times 5 \text{ mm}^3$ length. Powder $\sim 0.05 \text{ mm}$ particle size was used for measuring relative quantum efficiencies (RQE) of the samples. The RQE outputs at different temperatures were roughly evaluated by using a tungsten lamp with optical selective filters providing a luminescence excitation in the range 400–600 nm. The detector is a photomultiplier FEU-62 with maximum of the spectral sensitivity around 700–750 nm. The photomultiplier was

attached to a low-disperse prism monochromator UM-2 with spectral slit width adjusted in such a way that the whole range of the Cr^{3+} emission from ca. 660 to 750 nm could be covered. A difference in signal before and after switching on the lamp was admitted to be proportional to the RQE of the Cr^{3+} luminescence of each sample.

The photoluminescence spectra were taken in the range 200–1,000 nm at different temperatures. Selective-excitation spectra and selective-luminescence spectra were scanned at room temperature and 77 K using a 200 W high-pressure Xenon arc lamp and a 300 W quartz halogen lamp as exciting light sources in the 250–450 and 400–700 nm ranges, respectively. The light passes through a water filter and is adjusted on the entrance slit of a 0.5 m grating monochromator. The fluorescence emitted from the front surface of the sample was focused on the entrance slit of a MDR-23 grating monochromator. The outgoing light was detected by a photomultiplier FEU-100 attached to the exit slit of the monochromator. In the spectral range of Cr^{3+} R-lines the photoluminescence spectra were measured with spectral slit width not exceeding ca. 0.7 Å. The amplified signal was recorded with a strip-chart recorder. For further purposes spectral curves were scanned, digitized, and corrected for spectral response of the spectroscopic system using a standard lamp.

The samples preparation and measuring of polarized optical absorption spectra were performed as described by Taran et al. (2003). The diameter of the measuring spot did not exceed 500 μm . Spectra are normalized to 1.0 cm thickness.

Thermal treatments were performed at temperatures from 200 to 1,300°C with a pot furnace powered by an electronic device providing a temperature stabilization $\pm 10^\circ\text{C}$.

Results and discussion

In addition to the microprobe data of Taran et al. (2003) impurity contents of the topazes K1–K5 were determined by quantitative atomic emission analysis. As will be shown below, all observed photoluminescence characteristics of the topazes studied are caused by Cr^{3+} ions, whose concentrations (wt%) in the samples are as follows:

K1 (violet)	K2 (yellow-rose)	K3 (orange)	K4 (yellow-rose)	K5 (colorless)
0.03	0.05	0.03	0.015	0.002

It should be pointed out that besides chromium they contain some other transition metal ions of concentrations, except iron, significantly lower than that of chromium. However, as we found, these elements do not affect the luminescence characteristics of the samples.

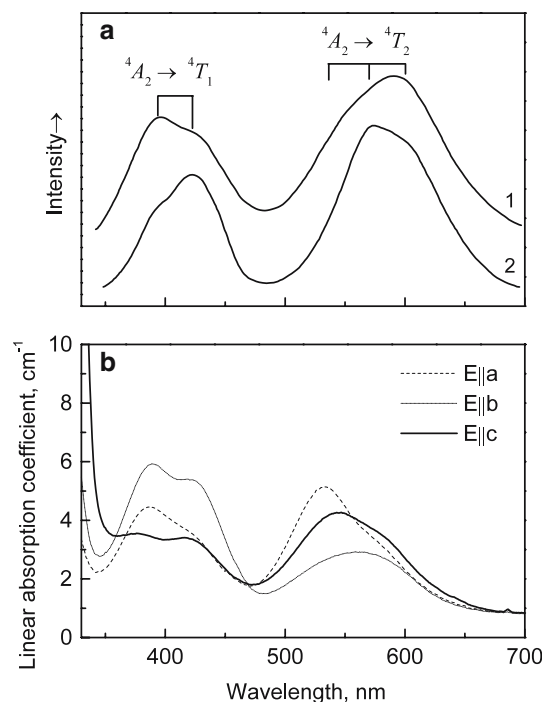


Fig. 1 **a** Selective-excitation spectra of Cr^{3+} ions in violet topaz K1 for emission monitored in 1 682.4 nm line (77K) and 2 broad band at 715 nm (room temperature); **b** polarized optical absorption spectra of topaz K1 at room temperature

Excitation spectra

Selective-excitation spectra of Cr^{3+} in sample K1¹ are shown in Fig. 1a. The two broad bands around 410 and 580 nm in the excitation spectra are undoubtedly due to the spin-allowed dd transitions of Cr^{3+} in sixfold coordination, i.e., due to the transitions ${}^4A_2 \rightarrow {}^4T_1$ and ${}^4A_2 \rightarrow {}^4T_2$, respectively. Note that the maxima in the selective-excitation spectrum are close to the maxima of the spin-allowed bands in the Cr^{3+} absorption spectra of this topaz (Fig. 1b).

The full-width at half-magnitude (FWHM) of the ${}^4A_2 \rightarrow {}^4T_1$ and ${}^4A_2 \rightarrow {}^4T_2$ bands (Fig. 1a) is rather large, i.e., at 300 K (for emission monitored in 715 nm) it is about 4,500 and 3,300 cm^{-1} and at 77 K (for emission monitored in 682.4 nm line) 4,100 and 2,600 cm^{-1} , respectively. These data support a multi- Cr^{3+} center model of topaz (Taran et al. 2003). In ruby, $\alpha\text{-Al}_2\text{O}_3:\text{Cr}^{3+}$, for instance, which is a typical single- Cr^{3+} center system, the FWHM of the ${}^4A_2 \rightarrow {}^4T_2$ band is only about 2,000 cm^{-1} (Maiman et al. 1961; Taraschan 1978). In mullite ceramics which are typical

¹Although the results obtained are measured on different samples, K1–K6, their luminescence characteristics are found to be qualitatively practically identical differing, due to different chromium contents, only by intensity of the emission. As will be shown below, due to somewhat different state of chromium in differently colored samples (valence, clustering), relatively weak differences were observed only in kinetics of thermal transformations of chromium-bearing luminescence centers.

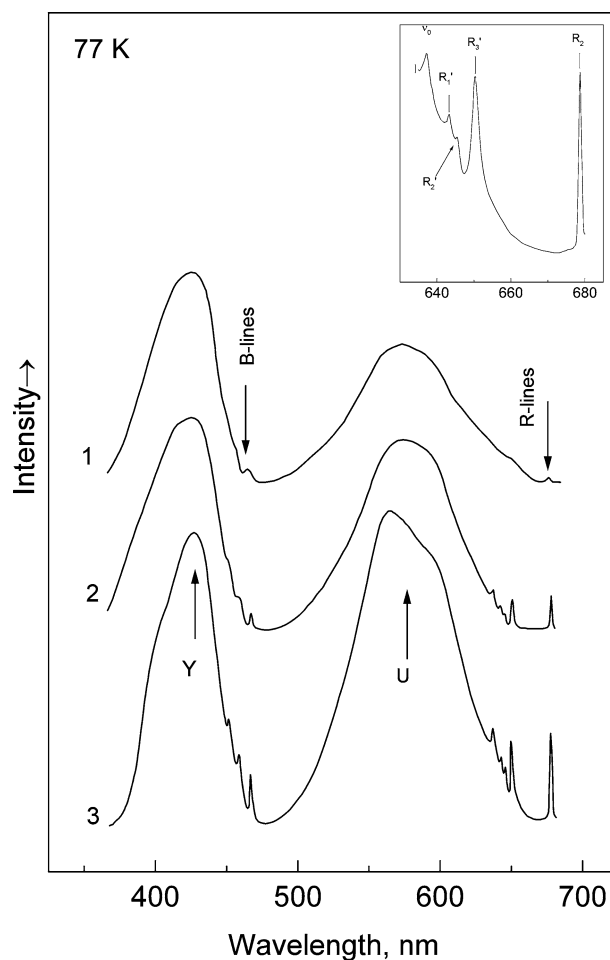


Fig. 2 Selective-excitation spectra of Cr^{3+} of orange topaz K1 annealed for 1.5 h at 1 1,000°C, 2 1,100°C, and 3 1,150°C. The spectra were recorded at 77 K in emission line 682.4 nm. Enlarged part of the spectrum 3 in the range of ${}^4A_2 \rightarrow {}^2T_1$ transition is shown in the inset. ν_0 , R- and B-lines see text

examples for multi- Cr^{3+} centers the FWHM is about 4,900 cm^{-1} (Wojtowicz and Lempicki 1988) and, hence, more than twice larger than in ruby.

Thermal annealing of the samples changes significantly the excitation spectra. A weak line system appears in the region 450 and 650 nm (Fig. 2). It is observable only after annealing the sample at least at 1,000°C for 1–1.5 h. The lines become stronger and more distinct after annealing at temperatures higher than 1,100°C. This development can also be tracked by significant changes in the luminescence spectra where the emission from two of the three mentioned non-equivalent Cr^{3+} complexes gradually decreases so that after annealing at 1,150°C only one type of the Cr^{3+} complexes is retained (see below).

The narrow lines observed in the excitation spectra of the annealed topaz K1 (Fig. 2) are characteristic for many chromium-bearing crystals. They are attributed to Cr^{3+} transitions from 4A_2 to the excited states 2E , 2T_1 , and 2T_2 (e.g., Fairbank and Klauminzer 1973; Sviridov et al. 1976). Spin-orbit interaction admixes 4T_1 - and

4T_2 -states having the same spin multiplicity as the ground state to the states 2E , 2T_1 , and 2T_2 . In absorption spectra, this causes an intensification of the respective absorption lines due to partial relaxation of the spin-multiplicity rule for the intercombinational ($\Delta S=1$) electronic transitions ${}^4A_2 \rightarrow {}^2E$, ${}^4A_2 \rightarrow {}^2T_1$, and ${}^4A_2 \rightarrow {}^2T_2$. In the excitation spectra of topaz these transitions are much more intense than in $\alpha\text{-Al}_2\text{O}_3\text{:Cr}^{3+}$ with comparable chromium content. The stronger intensity in topaz might be caused by a powerful admixing of the 4T_1 and 4T_2 states to the spin-forbidden ones. This seems to be reasonable because of the high distortion of the crystal field at the Cr^{3+} sites in topaz which is evident from the relatively strong splitting of 2E -, 2T_1 -, and 2T_2 -levels in excitation luminescence spectra. It should be noted that in the Cr^{3+} spectra of annealed topazes the splitting of the 2E -doublet to R_1 - and R_2 -lines, of the 2T_2 -triplet to R'_1 -, R'_2 -, and R'_3 -lines and of the 2T_1 -triplet to B_1 -, B_2 -, B_3 -lines are comparable with those of tetragonal and rhombic centers in MgO:Cr^{3+} (Fairbank and Klauminzer 1973). In the excitation spectra of all annealed topazes an additional line ν_0 appears at $15,694\text{ cm}^{-1}$ in the range of the ${}^4A_2 \rightarrow {}^2T_1$ transition (inset Fig. 2). We suppose that ν_0 is a zero-phonon line (ZPL) of the vibronic 4T_2 -band. Spectral position and assignment of the bands and lines observed in the excitation spectra of the annealed topaz K1, registered at 77 K at emission in the R_1 -line, are summarized in Table 1.

Luminescence spectra

Steady-state photoluminescence spectra of Cr^{3+} in natural light-violet topaz K1 excited at $\lambda_{\text{exc}} = 546\text{ nm}$ (4T_2 -band) and $\lambda_{\text{exc}} = 365\text{ nm}$ and registered at 300 and 77 K

Table 1 Wavelength, energy and assignment of bands and lines of Cr^{3+} excitation spectra in topaz K3 annealed at $1,150^\circ\text{C}$, measured at 77 K at emission in R_1 -line at 682.4 nm ($14,652\text{ cm}^{-1}$) (cf. Fig. 2)

Band	Wavelength (nm)	Energy (cm^{-1})	Assignment
V	262	38,168	${}^4A_2 \rightarrow {}^4T_1$ (4P)
Y	392	25,510	${}^4A_2 \rightarrow {}^4T_1$ (4F)
	427	23,419	
B_3	450.8	22,183	${}^4A_2 \rightarrow {}^2T_2$ (2G)
B_2	458.0	21,834	
B_1	466.3	21,445	
U	560	17,857	${}^4A_2 \rightarrow {}^4T_2$ (4F)
	590	16,949	
ν_0	637.2	15,694	${}^4A_2 \rightarrow {}^4T_2$ (4F)
R'_1	645.3	15,497	${}^4A_2 \rightarrow {}^2T_1$ (2G)
R'_2	643.5	15,540	
R'_3	650.3	15,378	
R_2	678.2	14,745	${}^4A_2 \rightarrow {}^2E$ (2G)
R_1	682.4	14,654	

V is not shown in Fig. 2

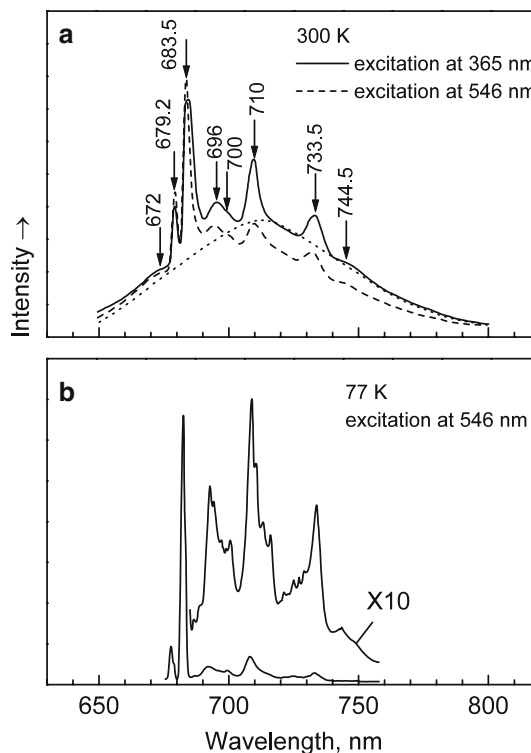


Fig. 3 Steady-state fluorescence spectra of Cr^{3+} in light-violet topaz K1: **a** recorded at room temperature using different wavelengths of excitation, 365 and 546 nm. Overlapped by the narrow-line spectrum the ${}^4T_2 \rightarrow {}^4A_2$ emission band is tentatively indicated by the dotted line; **b** recorded at liquid nitrogen temperature and at excitation 546 nm

are shown in Fig. 3. The room temperature spectrum (Fig. 3a) consists of several lines having different line width. They superimpose a broad unstructured band with maximum at around 715 nm ($\sim 14,000\text{ cm}^{-1}$) assigned to the electronic ${}^4T_2 \rightarrow {}^4A_2$ transition of Cr^{3+} . At 77 K the line spectrum (Fig. 3b) consists of an intense doublet at 682.4 and 678.2 nm. Such doublet, i.e., a relatively intense R_1 -line and partly “frozen out” R_2 -line is characteristic for Cr^{3+} and is caused by the spin-forbidden ${}^2E \rightarrow {}^4A_2$ transition. Some of the weaker and broader bands at higher wavelengths (see spectrum “ $\times 10$ ”) are obviously phonon satellites of these later zero-phonon transitions, R_1 and R_2 . Because the satellite lines superimpose the broad band its maximum can only be estimated to be between 710 and 720 nm. However, as seen from the comparison of Fig. 2 with Fig. 3, the shape and the position of this broad band correspond to the ${}^4A_2 \rightarrow {}^4T_2$ absorption band mirror-inverted against the ZPL, ν_0 , at $15,694\text{ cm}^{-1}$. The Stoke’s shift in this case is $\sim 3,400\text{ cm}^{-1}$.

Our investigations have shown that in all topazes studied the structure of the steady-state luminescence spectra is approximately independent of color and composition of the samples when wavelength of exciting illumination and temperature is kept constant. Of course, due to the different Cr^{3+} content the intensity of the emission bands and lines varies from sample to

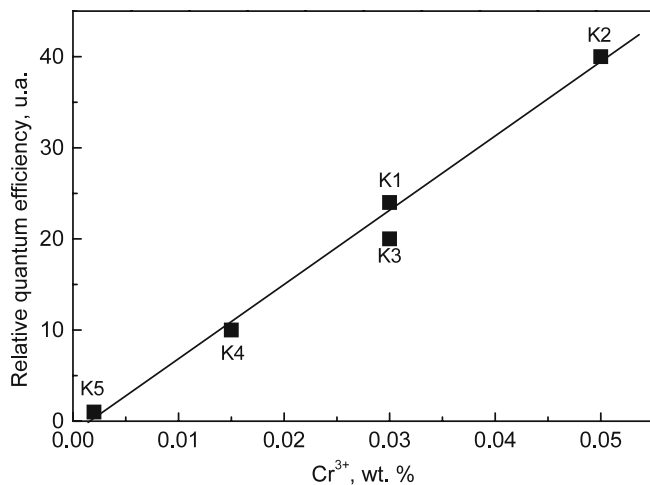


Fig. 4 Concentration dependence of the relative quantum efficiency of Cr^{3+} photoluminescence in natural topazes K1–K5. The relative quantum efficiency values are normalized to the value of the relative quantum efficiency of colorless topaz K5, the minimal among all samples studied, K1–K5

sample. Besides, they significantly increase after a thermal treatment.

The integral intensity of the overall Cr^{3+} luminescence of the topazes K1–K5 was taken at 300 K and at excitation in ${}^4\text{T}_2$ -band (650–750 nm). It is plotted versus the chromium concentration obtained by atomic emission analysis and shown in Fig. 4. Except for topaz K3 there is an excellent linear dependence between luminescence intensity and chromium content. After annealing at 600°C, all five samples fit perfectly a linear dependence. This observation strongly evidences that in the natural samples chromium is partly in a valence state different from Cr^{3+} , which, however, transforms to Cr^{3+} at thermal treatment. This deduction is consistent with that of Taran et al. (2003). The fact that just topaz K3 “drops out” from the linear dependence corroborates this suggestion very well because in K3 a large portion of chromium is found to be different from the trivalent valence state (Taran et al. 2003).

With increasing annealing temperature the intensification of the above mentioned luminescence lines derived from ${}^4\text{A}_2 \rightarrow {}^2\text{E}$, ${}^4\text{A}_2 \rightarrow {}^2\text{T}_1$, and ${}^4\text{A}_2 \rightarrow {}^2\text{T}_2$ transitions is accompanied by a gradual narrowing of the broad spin-allowed Cr^{3+} bands in the excitation spectra (cf. Fig. 2). Thus, at monitoring in 682.4 nm emission line the FWHMs of the spin-allowed bands measured at 77 K decreases from 4,100 to 2,900 cm^{-1} (${}^4\text{T}_1$ -band) and from 2,600 to 2,300 cm^{-1} (${}^4\text{T}_2$ -band) in untreated samples and in samples annealed at 1,150°C, respectively. The narrowing can be explained by weakening and finally disappearing of certain spin-allowed

Cr^{3+} bands which originate from different Cr^{3+} centers and first of all contribute to the overall width of the ${}^4\text{A}_2 \rightarrow {}^4\text{T}_1$ and ${}^4\text{A}_2 \rightarrow {}^4\text{T}_2$ bands of the multiple Cr^{3+} centers in the spectra of the untreated topazes.² This observation serves as additional justification of the multi-center model of Cr^{3+} in topaz supposed by Taran et al. (2003). It evidences that annealing decreases the number of non-equivalent Cr^{3+} luminescence centers in the topazes investigated here (see below).

R-lines

At 300 K the photoluminescence lines and narrow bands of topaz K1 appear at 672, 679.2 nm (R_2 -line), 683.5 nm (R_1 -line), 696, 700, 710, and 733.5 nm (Fig. 3a). Decreasing the temperature from 300 to 77 K the luminescence spectra change and the ${}^4\text{T}_2$ -band which is present as a broad unstructured band at 300 K is completely “frozen out” (Fig. 3b). In contrast, all narrow lines, especially the R-lines, become stronger and are shifted by about ~1 nm to shorter wavelengths. However, $\Delta\text{R} = \text{R}_2 - \text{R}_1$ remains practically unchanged and a weak fine structure of the R-lines and the side-bands emerges. Wavelengths and energies of R-lines and side-bands in the luminescence spectrum of natural topaz K1 at 77 K and excitation in the ${}^4\text{T}_2$ band are compiled in Table 2.

The linewidth of the lines in the spectra of topazes is rather broad in comparison to the equivalent lines in other chromium-bearing minerals. For example, at excitation in the ${}^4\text{T}_2$ -band at 300 K the FWHM values of R-lines are around 60 cm^{-1} and at 77 K ca. 40 cm^{-1} , whereas in natural ruby the corresponding values are 10 and 1 cm^{-1} , respectively. Several different mechanisms may broaden the luminescence lines in topaz. The two most important ones are the general inhomogeneous broadening and the broadening due to the superposition of several non-equivalent centers of Cr^{3+} . The first mechanism can be observed in diluted single-center systems especially in natural crystals. Structural defects like point defects, anisotropic defects, dipole defects, aggregates of impurity ions, dislocations, boundaries of microblocks, micropores, etc., may result in local elastic deformations around the luminescence centers. Especially defects allocated near crystal surfaces or phase boundaries are effective. Their relaxation by annealing causes significant narrowing of the luminescence lines and is commonly used as a routine procedure to improve, for example, solid-state laser materials (e.g., Kaminskii 1986).

The second mechanism, i.e., broadening due to line overlapping caused by non-equivalent Cr^{3+} centers seems to be a characteristic feature of the luminescence spectra of the Cr^{3+} -bearing topazes studied here. As already assumed by Schott et al. (2003) and Taran et al. (2003) the non-equivalent centers are Cr^{3+} ions with different (O,OH,F)-ligand surroundings. At this juncture the results of Akizuki et al. (1979) should be mentioned.

²We could not observe such narrowing of the spin-allowed bands of Cr^{3+} in optical absorption spectra (Taran et al. 2003) because at high-temperature annealing the samples become non-transparent (foggy) and, thus inappropriate for optical absorption measurements.

Table 2 Wavelengths λ and wavenumbers $\bar{\nu}$ of R-lines and side-bands in the Cr^{3+} luminescence spectrum of natural topaz K1 at 77 K and excitation in the ${}^4\text{T}_2$ band, 546 nm. The R_1 - and R_2 -values are obtained by curve fitting

	λ (nm)	$\bar{\nu}$ (cm^{-1})	$\Delta\bar{\nu}$ (cm^{-1a})	λ (nm)	$\bar{\nu}$ (cm^{-1})	$\Delta\bar{\nu}$ (cm^{-1a})
R_2	677.6	14,758		700	14,286	368
	678.2	14,745		708	14,114	540
	679.4	14,719		710	14,085	569
R_1	681.8	14,667		713	14,025	629
	682.4	14,654		716	13,966	688
	683.5	14,630		721	13,870	784
	686.0	14,577	77	725	13,793	861
	688.0	14,535	119	727	13,755	899
	692.0	14,451	203	729	13,717	937
	693.0	14,430	224	733	13,643	1,011
	697.0	14,347	307	743	13,459	1,195
	698.3	14,320	334			

^aMeasured relatively to the lowest zero phonon peak R_1 at $14,654 \text{ cm}^{-1}$: $\Delta\bar{\nu} = (\bar{\nu}_{\text{R}_1} - \bar{\nu})$

The authors showed that different sectors of growth in prismatic crystals of topaz from Ouro Preto differ in (OH,F)-ordering and, therefore have different symmetries, orthorhombic, monoclinic, or triclinic in $\{001\}$, $\{hk0\}$, or $\{hkl\}$ sectors, respectively. Thermal treatment at 950°C for 4 h of the samples gave rise to OH, F-disordering leading to an orthorhombic symmetry in all growth sectors.

An interesting observation is the broadening and the intensity variation of some luminescence lines when exciting with different wavelengths. For K1 and K6 topazes this is shown in Fig. 5. The excitation at 365 nm causes a significant broadening of R_1 -line luminescence in comparison with the excitation at 435 nm (${}^4\text{T}_1$) or at 546 nm (${}^4\text{T}_2$) (FWHM values are 95, 60, and 60 cm^{-1} , respectively). For R_2 -line FWHM value is practically independent of wavelength of excitation, remaining nearly 55 cm^{-1} . Simultaneously, the intensity of the side-bands at 710 and 734 nm is

noticeably higher when excited at 365 nm than at 546 nm (Fig. 3a). The intensity dependence of some luminescence lines on the exciting wavelength was also observed at room temperature by Gaft et al. (2003). Liquid nitrogen temperature luminescence spectra, however, do not show such effects. Although we cannot explain this observation in detail it may be caused by the tendency of chromium ions to form weakly coupled clusters if present in sufficient concentration (e.g., Imbusch 1967). Then, luminescence lines of Cr^{3+} in such clusters may be subject to a weak splitting seen as additional broadening of the lines. The spectrum of deep-violet topaz K6 with the highest chromium content, which shows stronger broadening of R_1 -line than that of topaz K2 (Fig. 5) seems to support this idea. Existence of Cr^{3+} -pairs and/or clusters in natural topazes is in agreement with weak and broadened EPR signals of Cr^{3+} in natural topazes with a high enough chromium concentration (Schott et al. 2003).

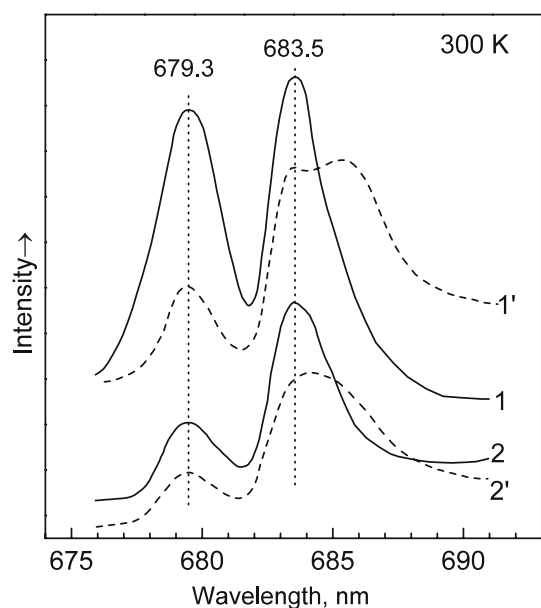


Fig. 5 Structure of luminescence R-lines in the spectra of K6 (1,1') and K1 (2,2') excited at 546 nm (1,2) and 365 nm (1',2'). The spectra were measured at room temperature

${}^4\text{T}_2$ -band

As shown in Fig. 6, increasing the temperature from 77 to 500 K both R-lines and side-bands broaden and weaken, so that at 500 K the luminescence spectrum consists of a single broad structureless band which maximum shifts from 715 nm at room temperature to $\sim 700 \text{ nm}$ at 500 K. Temperature-induced weakening of R-luminescence cannot be explained by the mechanism of resonant non-radiative decay of ${}^2\text{E}$ -level because the activation energy, E_{act} , of such a process is too high. In ruby, for instance, E_{act} is $\sim 8.9 \text{ eV}$. Perlin et al. (1970) studied this question theoretically and showed that at low temperatures the probability of a non-radiative tunneling decay of the excited $\text{Cr}^{3+} {}^2\text{E}$ -level is negligible in comparison with the probability of the radiative electronic transition ${}^2\text{E} \rightarrow {}^4\text{A}_2$. On the other hand, due to quick electronic transitions between ${}^2\text{E}$ and ${}^4\text{T}_2$ with increasing temperature the population of the short-lived ${}^4\text{T}_2$ -level increases which results in a decrease of the ${}^2\text{E}$ -state life time. Thus, the probability of radiative ${}^4\text{T}_2 \rightarrow {}^4\text{A}_2$ electronic transition increases. Therefore, the temperature-induced weakening of R-line luminescence should be accompanied by an intensification of the ${}^4\text{T}_2$ -

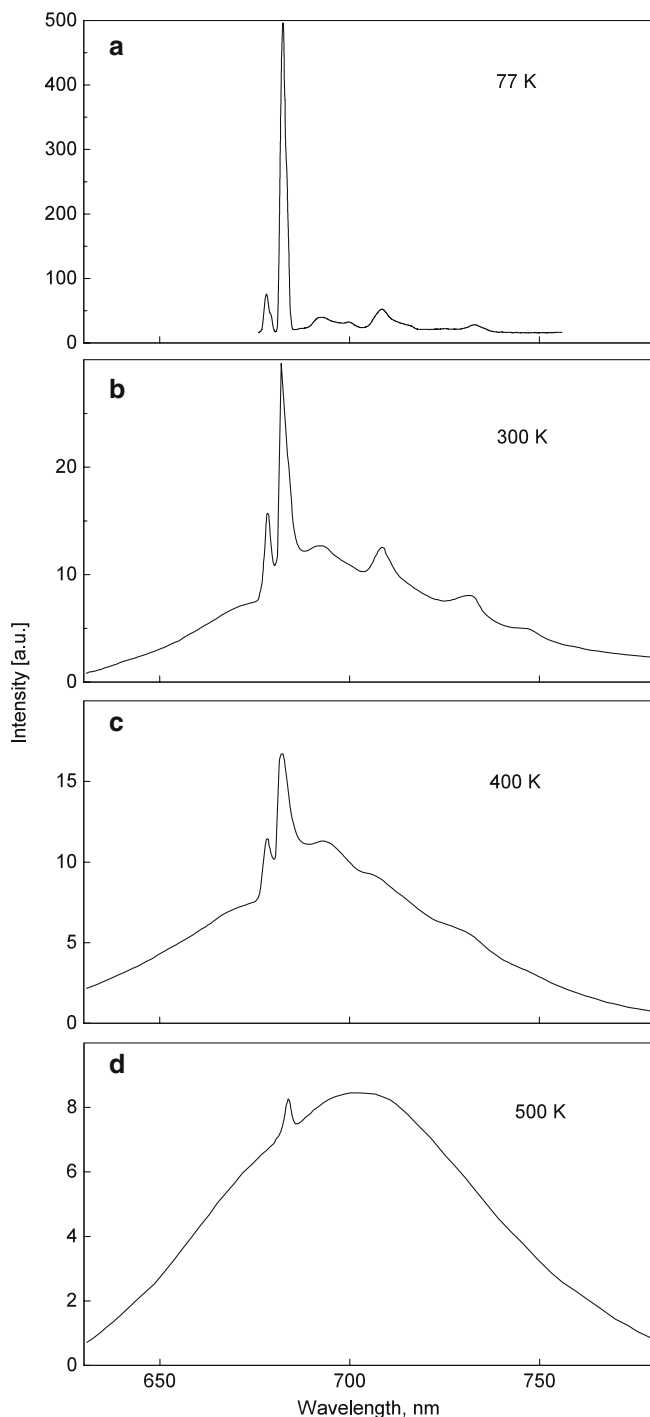


Fig. 6 Emission spectra of topaz K6 at 77 K (a), 300 K (b), 400 K (c), and 500 K (d), excited at 546 nm

band luminescence and the overall quantum efficiency of R- and 4T_2 -luminescence should remain nearly constant at temperatures increasing up to ~ 700 K (Kisliuk and Moore 1967).

The probability of thermal excitation of electron from 2E_2 to 4T_2 significantly depends on the difference, ΔE , between the 4T_2 - and 2E_2 -levels. In ruby, for instance, the 4T_2 -multiplet is $\sim 2,300$ cm^{-1} above the 2E

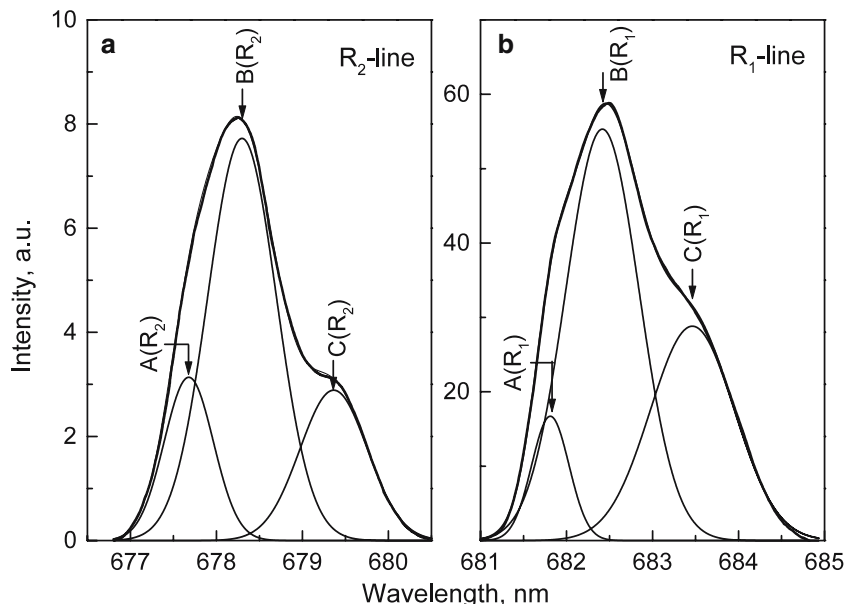
state (Kisliuk and Moore 1967) and at ~ 300 K it is not populated (called “strong crystal field case”). The observed luminescence is caused only by ${}^2E \rightarrow {}^4A_2$ transitions. The equilibrium between 4T_2 - and 2E -states in ruby can be reached only at temperatures higher than 400 K and, therefore, only at these temperatures the spectra are a superposition of both ${}^2E \rightarrow {}^4A_2$ and ${}^4T_2 \rightarrow {}^4A_2$ transitions (Gerlovin and Tolstoy 1975; Kisliuk and Moore 1967). In alexandrite ΔE is ~ 800 cm^{-1} (Kaminskii 1986) and in emerald ~ 400 cm^{-1} (Kisliuk and Moore 1967). Therefore, at room temperature the 4T_2 - and 2E -states in these two crystals are in thermal equilibrium (called “intermediate crystal field case”) and even at room temperature the spectra of alexandrite and emerald are a superposition of both ${}^2E \rightarrow {}^4A_2$ and ${}^4T_2 \rightarrow {}^4A_2$ transitions. In topaz such equilibrium also takes place at room temperature and in the luminescence spectra taken at 300 K the R-lines, their vibrational satellites, and the 4T_2 -band are distinct (Fig. 3a). This suggests that ΔE in topaz is not too large which allows for a mixing of the two excited states 2E and 4T_2 . By analogy with Mazurak (1994), ΔE -value in topaz was estimated using a single configuration coordinate diagram built up on experimental data obtained. We found that energy distance between the states 4T_2 and 4A_2 of Cr^{3+} ion in topaz is $1,050 \pm 50$ cm^{-1} that corresponds to a medium crystal field strength.

Non-equivalent chromium sites

As shown in Fig. 7, at 77 K both the R₂- and R₁-line could be fitted by three components denoted as A(R₂), B(R₂), C(R₂) and A(R₁), B(R₁), C(R₁), respectively. The distance between R₂ and R₁ in the doublets A(R₂,R₁), B(R₂,R₁), and C(R₂,R₁) is ~ 90 cm^{-1} and independent of the chromium concentration. The three doublets A(R₂,R₁), B(R₂,R₁), and C(R₂,R₁) are, therefore, attributed to non-equivalent Cr^{3+} centers having a ligand surrounding with different portions of F and OH. The fact that the shape of the R-lines at low temperatures does not change from sample to sample and does not depend on the chromium content evidences stable Cr^{3+} centers at definite structural sites in topaz. V^{4+} -EPR data taken from Brazilian topazes (Schott et al. 2003) also revealed a different F/OH/O composition of the vanadium coordination. Assuming that chromium and vanadium substitute aluminum complexes like $[\text{CrO}_4\text{F}_2]^{7-}$, $[\text{CrO}_4\text{OH,F}]^{7-}$, and $[\text{CrO}_4(\text{OH})_2]^{7-}$ might be formed. Further, beside similar Dq and splitting values of their 2E levels the three non-equivalent Cr^{3+}

Center	R ₁ (cm^{-1})	R ₂ (cm^{-1})	ΔR (cm^{-1})	FWHM (cm^{-1})
A	14,667	14,758	91	14
B	14,654	14,745	91	17
C	14,630	14,719	89	20

Fig. 7 Curve fitting of the fine-structured R_1 - (a) and R_2 -emission line (b) taken at excitation in maximum of ${}^4A_2 \rightarrow {}^4T_2$ absorption band ($\lambda_{\text{ex}} = 546 \text{ nm}$) and 77 K of topaz K2



centers exhibit at 77 K the following spectroscopic parameters:

The difference $R_A - R_B$ and $R_B - R_C$ is 13 and $\sim 25 \text{ cm}^{-1}$, respectively, for both R lines. Such a large splitting of R-lines can be explained only by structurally different Cr^{3+} centers since the fine structure of Cr^{3+} R-lines due to the splitting of the ground state 4A_2 is much smaller. For instance, the ground state splitting in ruby is only 0.38 cm^{-1} and in emerald 1.8 cm^{-1} (Sviridov et al. 1976). To prove the non-equivalence of the Cr^{3+} centers in topaz as well as to elucidate their nature we took into account the capability of topaz to transform at high temperatures to mullite a priori assuming that the distribution of Cr^{3+} in topaz is equivalent to the one of aluminum.

Stuckey and Amero (1941) studied first the structural instability of topaz and concluded that the evaporation of fluorine at $850\text{--}900^\circ\text{C}$ is related to a transformation of the topaz structure ending up with mullite. Kurilenko (1962) asserted that structural transformations in topaz take place already at $\sim 680^\circ\text{C}$ accompanied by the appearance of both amorphous silica and alumina. At $T \geq 1,000^\circ\text{C}$ the latter transforms to $\gamma\text{-Al}_2\text{O}_3$ acting as catalytic converter at further thermal transformations of topaz. Moreover, according to Kurilenko (1962) mullite appears only at or above $1,700^\circ\text{C}$. da Costa et al. (2000) did not observe any noticeable changes in the composition of topazes from Ouro Preto when annealing the samples up to $1,000^\circ\text{C}$. The mass loss occurred first at $1,200^\circ\text{C}$ which was attributed to the reduction of OH groups. The second mass loss started at $1,320^\circ\text{C}$ and was explained by the reduction of fluorine and the formation of mullite.

Therefore, transformations of the topaz structure at temperatures lower than $\sim 1,000^\circ\text{C}$ are questionable. However, it can be asserted that the structural transformation of topaz begins around $900\text{--}1,000^\circ\text{C}$ and that the final product is mullite. Keeping this in mind the

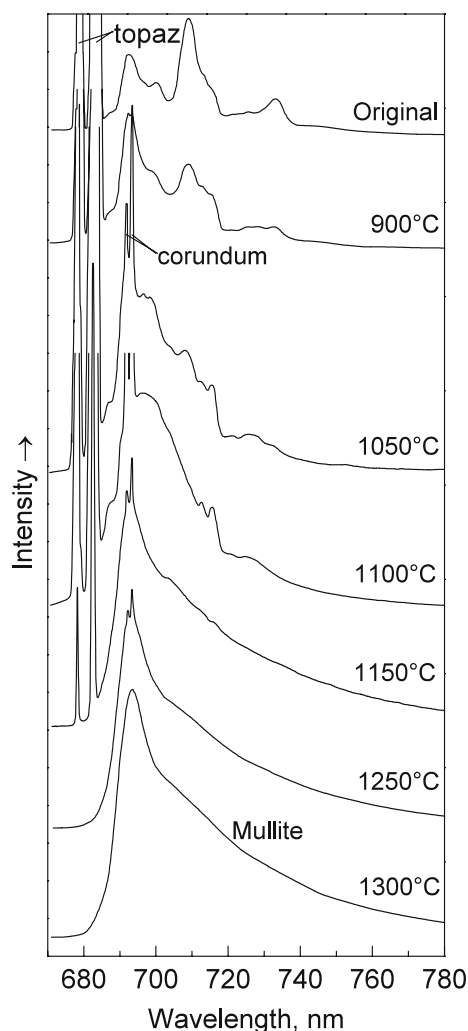


Fig. 8 Effect of thermal annealing (1.5 h at each temperature) on the luminescence spectra of yellow-rose topaz K2 excited at 546 nm. R-lines of Cr^{3+} in initial topaz and in the emerging corundum phases are designated. The spectra were recorded at 77K

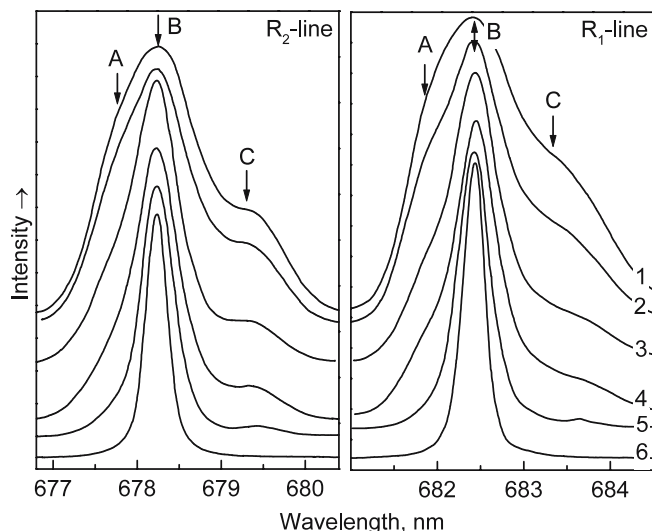


Fig. 9 Change of the shape of R-lines in luminescence spectra of topaz K2 after consequent annealing at different temperatures (°C): 1 900, 2 1,000, 3 1,050, 4 1,100, 5 1,150, 6 1,200. The annealing time at each temperature was 1.5 h. Spectra were recorded at 77 K and with excitation at 546 nm. Though the intensity of the R-lines increase with increasing annealing temperature more than one order of magnitude, here, they are shown normalized to nearly the same reference value

luminescence spectra of the thermally treated topazes K1–K5 will be interpreted in the following.

Annealing of a single crystal topaz was performed in air and in steps of 200°C up to 800°C. Above 800°C the step width was reduced to 50°C. The heating time was 1.5 h. For each annealing level a photoluminescence spectrum was taken at both 300 and 77 K and the intensity of R-lines was carefully monitored keeping the measurement parameters constant. In Fig. 8 the influence of annealing on the luminescence spectra and in Fig. 9 change of the shape of the Cr^{3+} R-lines are shown. Up to 900°C the shape of the spectra does not change besides a minor intensification of the side-bands. Annealing at temperatures higher than 950°C in the luminescence spectrum taken at 77 K lines at 693.4 and 691.9 nm appeared. They perfectly coincide with those observed in ruby (e.g., Görlich et al. 1966) and are, therefore, attributed to Cr^{3+} R-lines in a corundum phase. From the components A, B, C of the Cr^{3+} R-lines in topaz the components A and C exhibit an intensity loss when annealing the sample K2 at temperatures higher than 1,000°C (Fig. 9) whereas the intensity of the component B increases. This increase is not shown in Fig. 9 because for clarity all line intensities are normalized to nearly the same reference value. In reality, the concentration of B centers increases on the expense of A and C centers. Parallel to these processes at temperatures higher than $\sim 1,050^\circ\text{C}$ Cr^{3+} luminescence lines of Cr containing mullite appear and increase (Fig. 8). After annealing at 1,150°C the luminescence spectra of all topazes studied consist of a superposition of spectra of the residual topaz phase (B centers), the

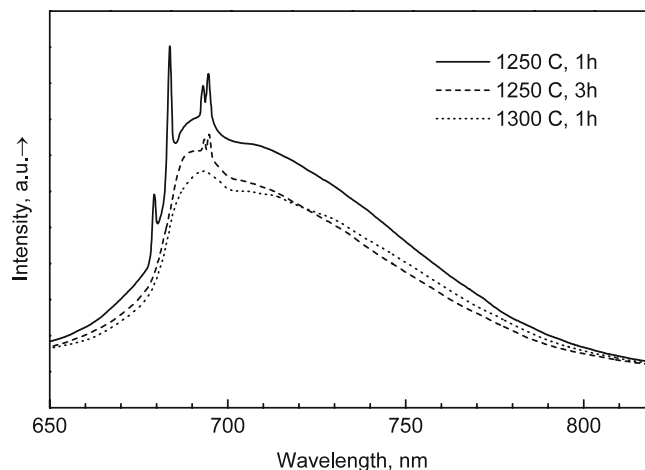


Fig. 10 Luminescence spectra of yellow-rose topaz K2 annealed at 1,250°C (1 h, solid line), 1,250°C (3 h, dashed line), and 1,300°C (1 h, dotted line). The spectra were recorded at room temperature at excitation in 546 nm

corundum and the mullite phase. The Cr^{3+} R-lines of the topaz phase disappear after annealing the sample 3 h at 1,250°C, those of corundum after annealing at 1,300°C (Fig. 10). At this temperature level the luminescence spectrum resembles strongly the spectrum of Cr^{3+} -doped mullite (cf. Wojtowicz and Lempicki 1988; Knutson et al. 1989; Piriou et al. 1996).

To confirm that topaz annealed at sufficient high temperatures transforms to mullite the excitation spectrum of K2 treated at 1,300°C has been compared with the excitation spectrum of a synthetic Cr^{3+} -doped mullite crystal (Fig. 11a). The polarized optical absorption spectra of the single crystal mullite are shown in Fig. 11b.³ Comparing Fig. 11a, b, we adhere to the statement that the main features of the Cr^{3+} absorption spectrum of mullite which was studied in detail by Ikeda et al. (1992) restore themselves in the excitation spectrum and is, therefore, caused by electronic transitions of Cr^{3+} . We assert that the excitation spectrum of K2 treated at 1,300°C is very close to that of mullite suggesting that the obtained phase is indeed mullite.

The annealing of the topazes had a significant influence on the intensity of the luminescence spectra. This can be established by intensity considerations of the R_1 -lines in topaz and in the forming of corundum phase (Figs. 8, 12). A weak intensification of the Cr^{3+} R_1 -line after annealing K2 at 400°C is obvious. This may be explained by change of valent states of chromium giving rise to increase of Cr^{3+} concentration (Taran et al. 2003).

At $\sim 950^\circ\text{C}$ the topaz structure alters. The comparison with the luminescence of ruby reveals that at this temperature in topaz a ruby-like phase arises. Further annealing strengthens the ruby phase combined with an increase of B centers and a decrease of A and C centers.

³As far as we are aware, polarized spectrum of Cr^{3+} -doped mullite is published for the first time.

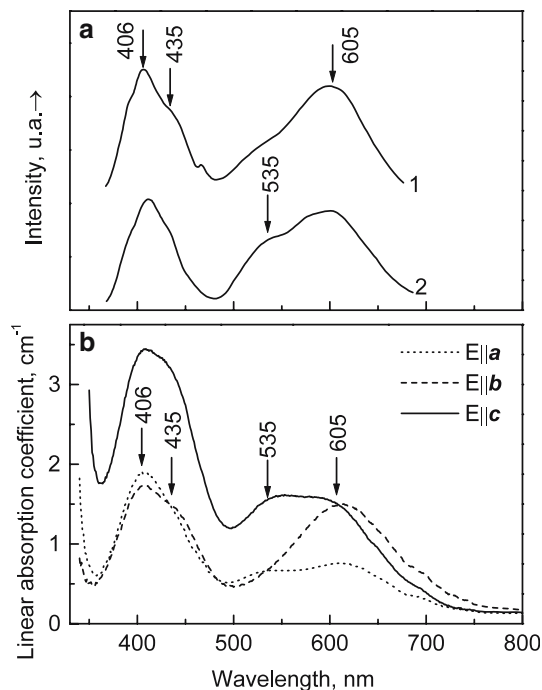
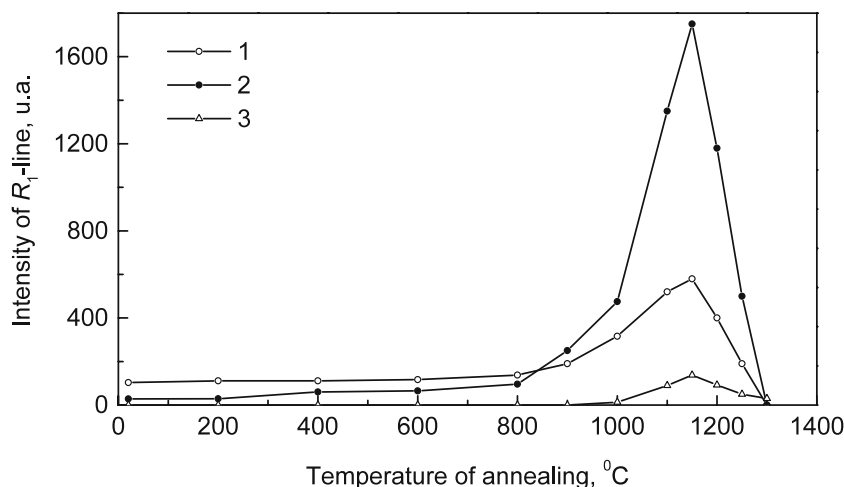


Fig. 11 **a** Excitation spectra of Cr^{3+} in a single-crystal mullite 1 and in a mullite phase generated in topaz K2 by annealing at 1,300°C (1 h) 2. The emission was monitored at 77 K in the range of 692 nm 1 and at 300 K in the range of 720 nm 2. **b** Polarized optical absorption spectra of Cr^{3+} in a synthetic single-crystal mullite containing 0.5 wt% Cr_2O_3 . The spectra were measured on two oriented slabs, ~0.80 and 1.13 mm thick, allowing measuring in three polarizations, $E||a$, $||b$, and $||c$, and then normalized to 1 cm thickness

These processes reach their maximum at 1,150°C. Parallel to the intensity increase of the R-lines at $14,564\text{ cm}^{-1}$ (R_1) and $14,745\text{ cm}^{-1}$ (R_2) a significant decrease of their FWHMs down to $\sim 6\text{ cm}^{-1}$ takes place and between 1,050 and 1,100°C additionally mullite arises. As seen from Fig. 8, further annealing heightens the concentration of mullite accompanied by a simultaneous decay of the B center in topaz and finally by a

Fig. 12 Effect of thermal treatment on the B center intensity of the R_1 -line in violet topazes K1 (1) and in yellow-rose topaz K4 (2). The R_1 -line intensity in the Cr^{3+} luminescence spectrum in Al_2O_3 (3) which emerged by heating of sample K1. The spectra were recorded at room temperature

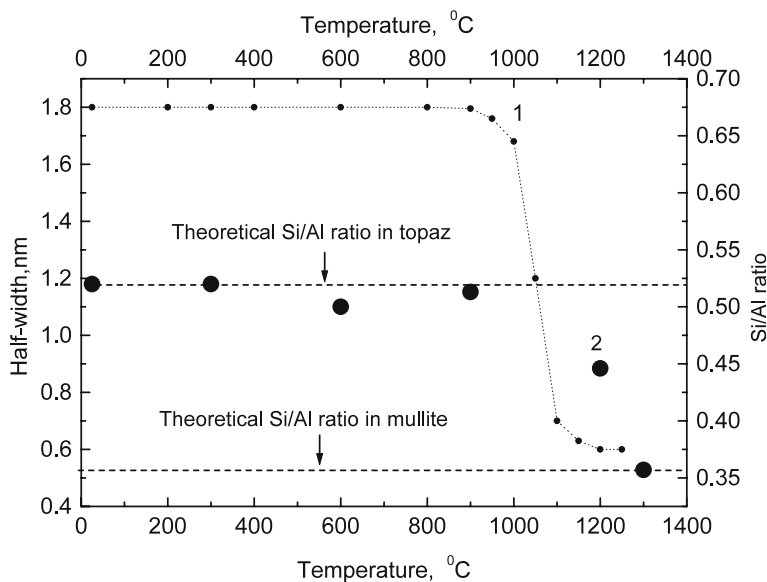


decay of the corundum phase. Strong intensification of R-lines between ca. 1,000 and 1,200°C (Fig. 12) may be explained by an increase of light scattering in topaz which loses its transparency and becomes foggy. In such a case multiple light scattering within the disperse optical medium and a longer light-pass occur increasing the overall absorption of the light in ${}^4\text{A}_2 \rightarrow {}^4\text{T}_2$ and ${}^4\text{A}_2 \rightarrow {}^4\text{T}_1$ bands of Cr^{3+} . This again results in an increasing luminescence in the R-lines. This fact is well known, i.e., due to the above-mentioned mechanisms powder usually has a much larger RQE than a perfect crystal from which it was ground (Smolskaya et al. 1985). Further, we believe that to some extent luminescence in annealed topazes increases due to the increase of isolated Cr^{3+} centers on the expense of $\text{Cr}^{3+}-\text{Cr}^{3+}$ pairs, for example.

Qualitatively the observed thermally induced changes in the Cr^{3+} luminescence (Fig. 13) is consistent with structural alterations in Brazilian topazes from Ouro Preto studied by da Costa et al. (2000). These authors showed that the low-temperature peaks of mass loss at $\sim 1,200^\circ\text{C}$ are caused by release of OH groups as H_2O or $\text{Si}(\text{OH})_4$. They established by infrared measurements that the absorption band at $3,460\text{ cm}^{-1}$ caused by OH vibrations completely disappears when the sample is annealed at $1,200^\circ\text{C}$ whereas this band is distinct in the spectra of natural untreated topaz samples from Ouro Preto. This undoubtedly evidences that the mass loss at $1,200^\circ\text{C}$ is caused by release of OH groups. The peaks of mass loss at $\sim 1,300^\circ\text{C}$ are believed to be caused by release of fluorine (da Costa et al. 2000). The product obtained after annealing at $1,380^\circ\text{C}$ is identified by these authors as mullite, $\text{Al}_6\text{Si}_2\text{O}_{13}$. They also assume that silicon releases from the structure as SiF_4 .

The thermally induced changes in topaz observed by luminescence spectroscopy agree with the changes established by da Costa et al. (2000) (Fig. 13). Narrowing of the R_1 -line between 900 and 1,100°C indicates a decrease of OH-coordinated A and C centers of Cr^{3+} (see above) and closely traces the change of Si/Al ratio in topaz related to the release of OH groups. R-lines of the

Fig. 13 1 The dependence of R_1 -line half-width on the annealing temperature in violet topaz K1. 2 Effect of the thermal treatment on the Si/Al ratio of an orange-yellow topaz from Ouro Preto, Brazil, according to the X-ray diffraction data of G.M. da Costa (2000). Both parameters decrease rapidly in the same temperature interval



topaz phase retain up to 1,250°C (Fig. 10) while the width of the R_1 -line changes negligibly in the thermal range 1,150–1,250°C (Fig. 13). From these we conclude that the B center, $\text{Cr}^{3+}\text{O}_4\text{F}_2$, retains up to ca. 1,250°C, while the A and C centers, $\text{Cr}^{3+}\text{O}_4\text{FOH}$ and $\text{Cr}^{3+}\text{O}_4(\text{OH})_2$ complexes, respectively, containing hydroxyl groups are less stable and disappear at annealing at 950–1,100°C. It should be mentioned that the transformation temperatures obtained by luminescence measurements (cf. Fig. 8) are noticeably lower than those obtained by X-ray diffraction phase analysis used by da Costa et al. (2000). This is due to the higher sensitivity of luminescence by which much lower concentrations of corundum or mullite phases during the thermal transformations of the topaz structure can be detected.

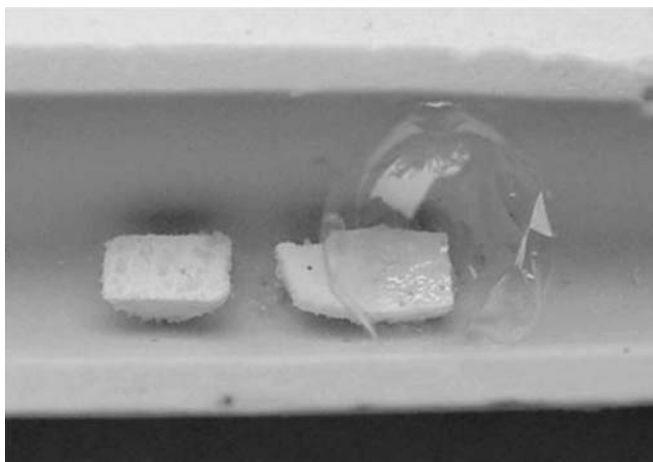


Fig. 14 Two pieces of topaz K2 in a ceramic holder after annealing at 1,300°C during 2 h and cooling down to room temperature. It is well seen that the samples, which were colored transparent gem-quality material have transformed to non-transparent milky-white stuff. There are a lot of bubbles on the surface of the left sample and one large bubble over the right one. We assume that the bubbles are formed by harden SiF_4 , released from the crystal during annealing

Interesting and not yet described is the fact that releasing of fluorine from the topaz structure by annealing may be seen visually. We found that crystals annealed at 1,300°C are usually covered by transparent lustrous bubbles. When cooled to room temperature (Fig. 14) they are very brittle and can be crushed down by a weakest touch. We did not study the bubbles in detail, but considering the temperature, 1,300°C, they are very likely formed by liquid SiF_4 exuded from crystals at its thermal transformation and hardened at cooling.

It should also be noticed that the thermally induced structural transformations in topaz proceed usually in an inhomogeneous way. Most of the samples studied which initially looked as rather homogeneously colored objects transformed at thermal annealing to zoned crystals wherein a part of them still retains transparency and pink Cr^{3+} -like color, whereas another part turned into a milky-white ceramics-like substance. It is essential that frequently but not always such transformations are structurally oriented, i.e., the ceramic-like zones are evidently related to certain crystal faces. This is well seen in Fig. 15 where a part of a topaz crystal cut perpendicular to the c -axis and annealed at 1,000°C during 2 h is still transparent and pink colored, whereas the transformed white zone is obviously related to one of the $\{001\}$ prism faces. At further annealing up to 1,300°C the whole crystal turns into a ceramics-like substance diagnosed afterwards by both luminescence and X-ray diffraction methods as mullite. These facts are very interesting and should be investigated in a further work.

Conclusions

Photoluminescence characteristics of variously colored Brazilian topazes are caused by Cr^{3+} entering the octahedral site of the topaz structure as $[\text{CrO}_4\text{F}_2]^{7-}$, $[\text{CrO}_4\text{OH}$,



Fig. 15 Two pieces of topaz K4, natural (*right*) and annealed during 1 h at 1,050°C (*left*). A part of the annealed sample transformed to non-transparent milky-white material. A distinct zone of the newly formed material is obviously related to one of the {001} prism face

$F]^{7-}$, and $[CrO_4(OH)_2]^{7-}$ complexes. This is experimentally proved by monitoring intensity and half-width of individual R-lines and studying thermal stability of the complexes at annealing in temperature range 200–1,300°C. As established, the two latter centers, $[CrO_4OH,F]^{7-}$ and $[CrO_4(OH)_2]^{7-}$, decay in the range 950–1,100°C that is accompanied by appearance of corundum phase. The most stable $[CrO_4F_2]^{7-}$ complex disappears after annealing at $\sim 1,250^\circ\text{C}$ and luminescence spectrum of the product obtained becomes identical to that of Cr^{3+} in mullite indicating that topaz transforms to mullite. These results clearly evidence that luminescence of Cr^{3+} may serve as a sensitive indicator of structural transformations and phase transitions in topaz.

Acknowledgments G.M. da Costa (Ouro Preto) kindly provided data on thermal treatment of topaz. The Deutsche Forschungsgemeinschaft, Bonn-Bad Godesberg, provided research stipendium to M.N.T. We are grateful to these individual and institution.

References

- Akizuki M, Hampar MS, Zussman J (1979) An explanation of anomalous optical properties of topaz. *Miner Mag* 43:237–241
- Burns RG (1993) *Mineralogical applications of crystal field theory*, 2nd edn. Cambridge University Press, Cambridge
- Da Costa GM, Sabioni ACS, Ferreira CM (2000) Imperial topaz from Ouro Preto, Brazil: chemical character and thermal behaviour. *J Gemm* 27:133–138
- Deutschbein O (1932) Die Linienhafte Emission der Chromphosphore. *Ann Phys* 14:729–754
- Fairbank WM, Klauminzer GK (1973) Tetragonal-field splittings of levels in $MgO:Cr^{3+}$. *Phys Rev B* 7:500–510
- Gaft M, Nagli L, Reinfeld R, Panczer G, Brestel M (2003) Time-resolved luminescence of Cr^{3+} in topaz $Al_2SiO_4(OH,F)_2$. *J Luminescence* 102–103:349–356
- Gerlovin IJ, Tolstoy NA (1975) Transition probability from the state 4T_2 in the ruby. In: Feofilov PP (ed) *Spectroscopy of crystals*. Nauka, Moscow, pp 353–356
- Görlich P, Karras H, Köttitz G, Lehmann R (1966) *Spectroscopic properties of activated laser crystals (in Russian)*. Nauka, Moscow
- Ikeda K, Schneider H, Akasaka M, Rager H (1992) Crystal-field spectroscopic study of Cr-doped mullite. *Am Miner* 77:251–257
- Imbusch GF (1967) Energy transfer in ruby. *Phys Rev* 153:326–337
- Kaminskii AA (1986) Laser crystals: progress and the main tendencies of investigations. In: Kaminskii AA (ed) *Physics and spectroscopy of laser crystals (in Russian)*. Nauka, Moscow, pp 5–61
- Kisliuk P, Moore CA (1967) Radiation from the 4T_2 state of Cr^{3+} in ruby and emerald. *Phys Rev* 160:307–312
- Knutson R, Liu H, Yen WM (1989) Spectroscopy of disordered low-field sites in Cr^{3+} :mullite glass ceramic. *Phys Rev* 40:4264–4270
- Kurilenko K (1962) The changing of topaz at annealing from 20 to 1250°C (in Russian). *Miner Sbornik* 16:395–399
- Maiman TH, Hoskins RH, D’Haenens IJ, Asawa CJ, Evtuhov V (1961) Stimulated optical emission in fluorescent solids. II. Spectroscopy and stimulated emission in ruby. *Phys Rev* 123:1151–1157
- Mazurak Z (1994) Luminescence and excited state 2E_g decay kinetics of Cr^{3+} in grossular $Ca_3Al_2(SiO_4)_3$. *Optic Mater* 3:89–93
- Parise JB, Cuff C, Moore FH (1980) A neutron diffraction study of topaz: evidence for a lower symmetry. *Miner Mag* 43: 943–944
- Perlin YuE, Zukerblat BS, Rosenfeld YuB (1970) The quantum efficiency of luminescence R-line of ruby. In: Grum-Grgimaylo SV, Feofilov PP, Skorobogatov BS, Cherepanov VI (eds) *Spectroscopy of crystals (in Russian)*. Nauka, Moscow, pp 90–95
- Piriou B, Rager H, Schneider H (1996) Time-resolved fluorescence spectroscopy of Cr^{3+} in mullite. *J Eur Ceram Soc* 16:195–201
- Schott St, Rager H, Schürmann K, Taran MN (2003) Spectroscopic study of natural gem quality “Imperial”- Topazes from Ouro Preto, Brasil. *Eur J Miner* 15:701–706
- Smolskaya KP, Parfianovich IA, Kolesnikova TA, Karpov YuM, Vasiliev GN, Shapiro BM (1985) The factors influencing on characteristics of oscillators and screens based on cesium iodine. In: Gurvich AM (ed) *Luminescence detectors and transformers of ionizing radiation (in Russian)*. Novosibirsk, Nauka, pp 81–95
- Stuckey JL, Amero JJ (1941) Physical properties of massive topaz. *J Am Ceram Soc* 24:89–92
- Sviridov DT, Sviridova RK, Smirnov YuF (1976) Optical spectra of transition metal ions in crystal (in Russian). Nauka, Moscow
- Taran MN, Tarashchan AN, Rager H, Schott St, Schürmann K, Iwanuch W (2003) Optical spectroscopy study of variously colored gem quality topazes from Ouro Preto, Minas Gerais, Brazil. *Phys Chem Miner* 30:543–555
- Tarashchan AN (1978) *Luminescence of minerals (in Russian)*. Naukova Dumka, Kyiv
- Wojtowicz AJ, Lempicki A (1988) Luminescence of Cr^{3+} in mullite transparent glass ceramics (II). *J Luminescence* 39:189–203